Plasma Physics and Controlled Fusion

PAPER

Numerical investigation of active control of tearing mode by magnetic coils and the role of Δ′

To cite this article: Yuling He *et al* 2021 *Plasma Phys. Control. Fusion* **63** 075015

IOP Publishing Plasma Physics and Controlled Fusion

Plasma Phys. Control. Fusion **63** (2021) 075015 (12pp) https://doi.org/10.1088/1361-6587/ac0110

Numerical investigation of active control of tearing mode by magnetic coils and the role of Δ'

Yuling He[1,2,*], Yueqiang Liu[3,*], Li Li[4], Xu Yang[5] and Guoliang Xia[6]

[1] Guangdong Provincial Key Laboratory of Quantum Engineering and Quantum Materials, School of Physics and Telecommunication Engineering, South China Normal University, Guangzhou 510006, People's Republic of China
[2] Guangdong-Hong Kong Joint Laboratory of Quantum Matter, South China Normal University, Guangzhou 510006, People's Republic of China
[3] General Atomics, PO Box 85608, San Diego, CA 92186-5608, United States of America
[4] College of Science, Donghua University, Shanghai 201620, People's Republic of China
[5] Chongqing Engineering Laboratory for Detection, Control and Integrated System, Chongqing Technology and Business University, Chongqing 400067, People's Republic of China
[6] CCFE, Culham Science Centre, Abingdon OX14 3DB, United Kingdom

E-mail: heyl@m.scnu.edu.cn and liuy@fusion.gat.com

Received 5 February 2021, revised 24 March 2021
Accepted for publication 13 May 2021
Published 2 June 2021

Abstract

Magnetic feedback stabilization of the tearing mode (TM) is numerically investigated, utilizing the MARS-F code (Liu *et al* 2000 *Phys. Plasmas* **7** 3681) for toroidal tokamak equilibria. With control coil configurations assumed in this study, magnetic feedback partially or fully stabilizes the TM, with either vanishing or finite equilibrium pressure. The best control is achieved by the combination of internal active coils and internal poloidal sensors. The internal and external tearing indices are evaluated for the close-loop system, based on the MARS-F computed mode eigenvalue and eigenfunction, respectively. In the absence of the favorable curvature effect, these two indices are real-valued and quantitatively agree well with each other. For the equilibrium with finite pressure gradient at the mode rational surface, the favorable average curvature effect becomes important and the close-loop tearing index also becomes complex-valued, partly due to interaction of the feedback system with the dissipative wall eddy current response. Isolating the inner layer and outer region response to magnetic feedback, with either proportional or proportional-derivative actions, allows to establish that feedback stabilization of the TM occurs mainly due to modification of the behavior of the external ideal solution, further confirming the analytic result reported in He *et al* 2021 *Phys. Plasmas* **28** 012504.

Keywords: active control, tearing mode, toroidal tokamak equilibria

(Some figures may appear in colour only in the online journal)

1. Introduction

The tearing mode (TM) is an important macroscopic instability affecting tokamak operations. Non-linear development of a TM creates magnetic islands [1] that limit the plasma performance, and in severe cases even induce plasma disruptions [2]. Furthermore, the neoclassical TM (NTM) can be triggered at sufficiently high plasma pressure, either with or without a finite sized seed island. The latter, observed in DIII-D experiments under international thermonuclear fusion reactor (ITER)-like conditions, appears to follow the classical drive mechanism for TM [3]. TM/NTM avoidance and/or control is an essential issue in ensuring successful and optimal tokamak operations.

* Authors to whom any correspondence should be addressed.

Analytic study of the TM stability often employs the asymptotic matching technique, where an inner layer (near the mode rational surface) problem with finite plasma resistivity is independently solved from the outer region where the plasma is treated as a perfectly conducting fluid [4]. The inner and outer solutions are then matched via the tearing index Δ', in order to determine the TM stability. The external tearing index, $\Delta'_{\rm ext}$, is defined as the logarithmic jump of the radial magnetic field perturbation across the rational surface for plasmas where constant-ψ approximation is valid. For more general cases, where the outer region solution has strong singularities with two independent branches that exhibit different fractional power-like asymptotic behavior, $\Delta'_{\rm ext}$ represents the ratio of small to large solutions [5]. The inner resistive layer solution yields $\Delta'_{\rm int}$ which depends on the mode eigenvalue [5–8]. The matching condition $\Delta'_{\rm ext} = \Delta'_{\rm int}$ gives the dispersion relation for the TM. One aspect of the present study is to numerically determine $\Delta'_{\rm ext}$ for toroidal plasmas, and more importantly to find out how magnetic feedback modifies $\Delta'_{\rm ext}$.

Theoretically, the stability of TM is known to sensitively depend on the local equilibrium pressure gradient within the resonant layer [9–12]. Reference [11] analytically calculated the sensitivity of Δ' to local flattening of the pressure profile near the resonant surface in a cylindrical model. This study was later extended to toroidal geometry in [13]. The effect of toroidal coupling on the tearing index is also numerically investigated [14–17], using the resistive magnetohydrodynamic (MHD) solver MARS-F [18] and the ideal shooting code T7 [15]. Reasonably good agreement was found over the range of parameters as reported in [17]. In this work, we again employ MARS-F and the local pressure flattening approach to compute the tearing index, but in the presence of magnetic feedback.

Feedback stabilization of MHD modes, in the presence of both plasma and wall resistivity, has been the focus of several recent studies [19–23]. Active control of MHD instabilities is generally an essential consideration for future tokamaks [24–26], such as ITER, chinese fusion engineering testing reactor (CFETR) and demonstration fusion reactor (DEMO). experiments in RFX-mod (operated in a circular cross-section ohmically heated tokamak configuration), where the $m/n = 2/1$ TM (m is the poloidal and n the toroidal Fourier harmonic numbers) is actively controlled as the $q = 2$ resonant surface approaches the plasma boundary, showed that the plasma disruption can be avoided [22]. The analytic study in a cylinder, reported in [23], shows that magnetic feedback can stabilize the resistive-plasma resistive wall mode, largely due to modification of the external tearing index.

This work focuses on numerical study of active control of the TM in toroidal plasmas, using 3D fields produced by magnetic coils as the actuator. We utilize the direct resistive MHD solver MARS-F, which has been extensively used for modeling active control of MHD modes by 3D fields [27–29] as well as the plasma response to externally applied 3D fields [30–32]. Being an eigenvalue solver, MARS-F provides both eigenvalue and eigenfunction of the TM in the presence of magnetic feedback. The eigenvalue will be used to derive the internal tearing index, whilst the eigenfunction will be used to evaluate the external tearing index. Both indices will be compared as we vary the feedback gain, in order to understand the relative role of magnetic control in the inner versus outer layer solutions via direct toroidal computations.

We point out that feedback control of the TM has been theoretically studied in several early works [19, 33, 34]. In particular, [33] provided a theoretical foundation for magnetic feedback control of the TM, by showing that a proportional feedback system can reduce the external tearing index to a negative value and thus stabilizes the mode. Reference [34] derived equations for the magnetic island evolution in the presence of an external source field (either feedback control field or error field) without directly invoking the feedback law. But the formulation can be easily incorporated into a system with feedback law to study active control of the TM. The main advances of our work in relation to the previous results are: (a) our work represents a toroidal realization of the TM control scheme envisaged in [19, 33, 34] with analytic cylindrical plasma models; (b) our work considers a more systematic approach (various combinations of active and sensor coil types, proportional as well as derive feedback actions) as long as the control aspect is concerned; (c) we recover both the outer and inner tearing indices from the external and internal solutions, respectively, from the MARS-F direct feedback modeling results, and show that these two tearing indices can indeed match; (d) we also compare feedback control of the TM with and without the favorable average curvature effect.

Section 2 briefly presents the computational model and plasma equilibria assumed in this study. Feedback stabilization of the TM, and the role of Δ', are reported in section 3 assuming an equilibrium with vanishing plasma pressure. A similar study is carried out in section 4, where we consider equilibria with finite pressure, with or without local flattening of the pressure profile near the mode rational surface. Conclusion is drawn in section 5.

2. Computational model and plasma equilibria

2.1. Computational model

This work focuses on feedback control of the linear TM. Linear toroidal resistive MHD code MARS-F is utilized for this purpose. Without considering equilibrium plasma flow, the linearized, single-fluid, resistive MHD equations read

$$\rho_0\hat{\gamma}\mathbf{v}_1 = -\nabla P_1 + \mathbf{j}_1\times\mathbf{B}_0 + \mathbf{J}_0\times\mathbf{b}_1 \tag{1}$$

$$\hat{\gamma}\mathbf{b}_1 = \nabla\times(\mathbf{v}_1\times\mathbf{B}_0) - \nabla\times\eta\mathbf{j}_1 \tag{2}$$

$$\hat{\gamma}P_1 = -\mathbf{v}_1\cdot\nabla P_0 - \Gamma P_0\nabla\cdot\mathbf{v}_1 \tag{3}$$

$$\mu_0\mathbf{j}_1 = \nabla\times\mathbf{b}_1 \tag{4}$$

where $\hat{\gamma} = \gamma + \mathrm{i}\omega_{\rm r}$ is the eigenvalue of the mode (γ and $\omega_{\rm r}$ being the mode growth rate and real frequency, respectively).

Quantities with subscript '0', ($\rho_0, \mathbf{B}_0, \mathbf{J}_0, \mathbf{P}_0$), denote the equilibrium plasma density, magnetic field, current and pressure, respectively. These equilibrium quantities are the solution to the force-balance Grad–Shafranov equation, solved by using an equilibrium code CHEASE [35]. Quantities with subscript '1' denote the corresponding first-order perturbed fields. All the perturbed quantities have toroidal mode number $n = 1$ as opposed to the equilibrium quantities that have toroidal mode number of $n = 0$. $\Gamma = 5/3$ is the ratio of specific heats. η is the plasma resistivity, which will be specified through a dimensionless quantity, the Lundquest number $S = \tau_R/\tau_A$, in this work. Here, $\tau_R = \mu_0 a^2/\eta$ is the resistive decay time of the plasma current, and $\tau_A = R_0\sqrt{\mu_0\rho_0}/B_0$ is the toroidal Alfven time (R_0 and a are the plasma major and minor radii, respectively).

A basic feedback law is applied to model active control of the resonant magnetic perturbation (RPM)

$$M_{sf} I_f = -G\psi_s \tag{5}$$

where M_{sf} is the mutual inductance between the feedback coil and the sensor loop. The magnetic sensor signal ψ_s is fed back to determine the current I_f flowing in the active coils. The dimensionless quantity

$$G = K_P\,(1 + \alpha\gamma\tau_F) \tag{6}$$

is the feedback gain, with K_P representing the overall gain amplitude. The parameter α defines the ratio of the derivative to proportional gains, with $\alpha = 0$ recovering the proportional (P) controller and $\alpha \neq 0$ yielding the proportional-derivative (PD) controller. τ_F is the L/R response time of active coils.

MARS-F directly solves the resistive MHD equations across the whole plasma column. The code thus does not directly compute the external tearing index, unlike T7 which employs the shooting method. For cases where the constant-ψ approximation holds, we evaluate Δ'_{ext} as the logarithmic jump of the radial field perturbation, based on the MARS-F computed TM eigenfunction

$$\Delta'_{ext} \equiv \frac{r\left[b'_{r,m}\right]_{r_s}}{b_{r_s,m}} \tag{7}$$

where $[f(x)]_y \equiv f(y+\delta) - f(y-\delta)$ is the jump value across a small layer width of 2δ to be numerically determined. $b_{r,m}$ is the perturbed radial magnetic field for the resonant poloidal harmonic m. r_s is the radial location of the resonant surface for the mode.

The internal tearing index, Δ'_{int}, is generally evaluated using the following expression which is valid for large aspect ratio circular plasma

$$\Delta'_{int}(\hat{\gamma}) = 2.12\,(1+g)\,\mathrm{A}(\hat{\gamma}\tau_A)^{5/4} \times \left[1 - \frac{1}{1+g}\frac{\pi}{4} D_R B(\hat{\gamma}\tau_A)^{-3/2}\right] \tag{8}$$

where $\hat{\gamma}$ is the close-loop eigenvalue computed by MARS-F. The correction factor $g \approx \left(\frac{\pi}{4} - 1\right) Q D_R$ was introduced in [30], with Q being inversely proportional to the ratio of specific heats [5, 6]. $\mathrm{A} \equiv (ns)^{-1/2}\left(1 + 2q_{r_s}^2\right)^{1/4} S^{3/4}$ and $B \equiv (ns)\left(1 + 2q_{r_s}^2\right)^{-1/2} S^{-1/2}$, with s and S being the magnetic shear and Lundquist number, respectively. n is the toroidal mode number assumed to be 1 in this study. The resistive interchange index, D_R, is typically a small negative number for a tokamak plasma, being roughly proportional to the plasma pressure gradient at the mode rational surface. For an equilibrium with vanishing plasma pressure or with locally vanishing plasma pressure gradient at the mode rational surface, we have $D_R = 0$ in equation (8) and the favorable average curvature stabilization effect thus disappears. The aforementioned two cases differ by the Pfirsch–Schluter inertial enhancement factor, $1 + 2q_{r_s}^2$, from the coefficients A and B. In other words, this inertial enhancement factor should be dropped for the pressure-less equilibrium.

Based on the MARS-F computed close-loop TM eigenfunction and eigenvalue, equations (7) and (8) are thus used to evaluate the external and internal tearing indices, respectively. A consistent evaluation procedure should result in the same value for both Δ'_{ext} and Δ'_{int}. More importantly, isolating both tearing indices from the MARS-F results allows us to understand to which degree magnetic feedback stabilization of the TM is due to modification of the external ideal solution. This aspect is also the focus of the present study, on top of direct demonstration of feedback stabilization of the TM by the MARS-F modeling.

2.2. Equilibria

Since equation (8) is strictly valid only for a large aspect ratio circular plasma, we shall consider such a plasma with MARS-F computations. We remark that it is certainly of more practical interest to consider a tighter aspect ratio plasma and possibly with plasma shaping effect as well (MARS-F close-loop modeling is capable of dealing with generic toroidal equilibria). However, equation (8) will then need modifications for quantifying the internal tearing index, e.g. by adding an *a-priori* unknown geometric correction factor to equation (8). In this work, we avoid this complication by choosing simple toroidal equilibria.

We consider a set of equilibria with aspect ratio of 10 and with a circular plasma boundary shape, surrounded by a resistive wall of also circular shape (figure 1). The wall is placed at $r_w = 1.4a$, with a wall time of $\tau_w = 10^4\tau_A$. For feedback control of the TM, we also consider a single set of active and sensor coils, both placed near the low field side mid-plane as shown in figure 1. The active coils are radially located either external ($r_f = 1.5a$) or internal ($r_f = 1.3a$) to the resistive wall. The poloidal angle coverage, normalized by π, of each active coil, is fixed at $\Delta\theta = 0.65$ for the equilibrium with vanishing plasma pressure and $\Delta\theta = 0.4$ for the finite pressure cases. Note that the coverage angle is chosen differently for different equilibria, to ensure the best control in each case in terms of minimizing the feedback gain. The sensor coils, measuring the radial or poloidal component of the magnetic field perturbation, is located at $r_s = 1.2a$ (i.e. internal to the wall).

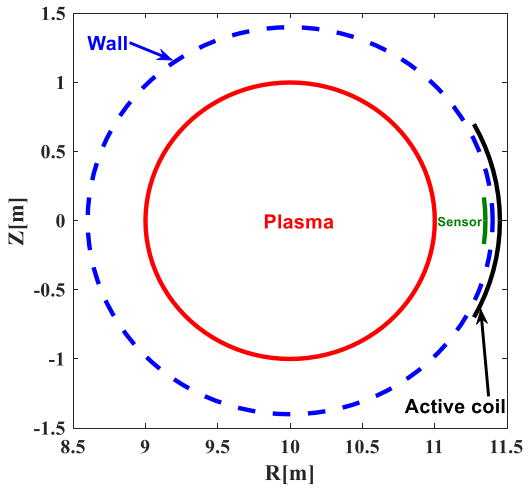

Figure 1. Feedback geometry on the poloidal plane, including the plasma boundary, the resistive wall, and a sketch of the active and sensor coils.

The plasma major radius is chosen to be $R_0 = 10$ m, and the vacuum toroidal field at the major radius is chosen to be $B_0 = 1$ T. The equilibrium current (the toroidal component) density and pressure profiles are specified as $J = J_0\left(1 - r^2\right)$ and $P = P_0\left(1 - r^2\right)^2$, respectively. The current amplitude, J_0, is constrained by the on-axis safety factor of $q_0 = 1.05$. The plasma resistivity is assumed to be uniform along the radial coordinate. Note that all equilibria are obtained by the fixed boundary equilibrium solver CHEASE [35], thus satisfying the MHD force balance.

As mentioned before, for the finite pressure case, we also consider another equilibrium pressure with local flattening of the profile near the mode rational surface, in our case the $q = m/n = 2/1$ surface. Examples of the equilibrium pressure and safety factor profiles, with or without local flattening, are shown in figure 2. The finite pressure cases have $\beta_N \equiv \beta\,[\%]\,a\,[m]\,B_0\,[T]/\,I_P\,[MA] = 0.65$, with β being the ratio of the volume averaged plasma pressure to the magnetic pressure, and I_P the total plasma current. For the equilibrium with local pressure flattening, the radial width of the flattened region is fixed at $\Delta r = 0.01$, well covering the resistive layer near the $q = m/n = 2/1$ rational surface in our case. Note that the q−profiles almost do not change for our equilibria while varying the plasma pressure. This is a useful property for comparative study of the TM control with different layer physics (i.e. with or without the favorable average curvature effect). Also note that the equilibrium parameters are chosen here such that there is a single rational surface inside the plasma for the $n = 1$ TM.

The open-loop TM stability, computed by MARS-F, is reported in figure 3 as we scan the plasma pressure up to the no-wall beta limit (∼1.6 in our case) for the onset of the $n = 1$ ideal kink instability. Within certain range of finite equilibrium pressure (and finite pressure gradient at the $q = 2$ surface), the TM has finite frequency for static equilibria, due to the favorable curvature stabilization [5]. With local flattening of the pressure profile near the $q = 2$ surface, the favorable curvature effect is removed. The mode becomes more unstable meanwhile the mode frequency always vanishes. We also note a sharp variation of the mode growth rate near $\beta_N = 0$. This is due to the Pfirsch–Schluter inertial enhancement factor as discussed before and also mentioned in [29]. The other interesting observation, which is not the focus of the present study though, is a significant increase of the TM growth as the plasma pressure approaches the no-wall beta limit. This is due to large increase of the tearing index associated with a pole at this limit [21].

For the close-loop study that follows, we choose equilibria (with or without local pressure profile flattening) at $\beta_N = 0.65$, where the favorable average curvature is sufficiently strong to induce finite mode frequency, while fixing the on-axis safety factor at $q_0 = 1.05$.

3. Close-loop TM stability and Δ′ for equilibrium with vanishing pressure

In what follows, we first directly compute the close-loop TM stability utilizing the MARS-F code, assuming proportional (P) or PD controller. Next, we investigate how magnetic feedback changes Δ' based on the MARS-F computed eigenvalue and eigenfunction. For plasma equilibria with vanishing plasma pressure (which we consider in this section), or with locally vanishing pressure gradient near the mode rational surface (to be considered in the next section), it is possible to evaluate the external tearing index based on the MARS-F computed mode eigenfunction. The procedure is illustrated below.

We consider the $m/n = 2/1$ harmonic of the perturbed radial magnetic field associated with the unstable TM, with one example shown in figure 4(a). (The MARS-F toroidal computations include 15 poloidal harmonics in total to ensure numerical convergence.) Note that this $2/1$ radial field component represents the global radial structure of the TM eigenfunction that includes both the inner and outer solutions, smoothly coupled via the direct MHD solver. In order to obtain the external tearing index, we need to take a proper jump of the radial derivative shown in figure 4(b), through the resistive layer of width 2δ. The key issue is the choice of δ. Although the radial field perturbation is regular across the layer, the radial derivative exhibits singular-like behavior near the $(q = 2)$ rational surface as expected [12]. More importantly, a finite jump in the radial derivative appears when we plot $\left[\partial b_{r,m/n=2/1}/\partial r\right]_{r_s} = \partial b_{r,m/n=2/1}/\partial r\big|_{r=r_s+\delta} - \partial b_{r,m/n=2/1}/\partial r\big|_{r=r_s+\delta}$ as a function of δ, as shown in figure 4(c). Note that there is a peak value (a generic feature for the TM eigenfunctions computed in this work) in the jump occurring at certain value δ_0, which can be assumed as a reference for separating the inner and outer regions, and thus for evaluating the external tearing index according to expression (7). We shall, however, perform more fine tuning of the layer width around δ_0 for calculating Δ', as explained later on.

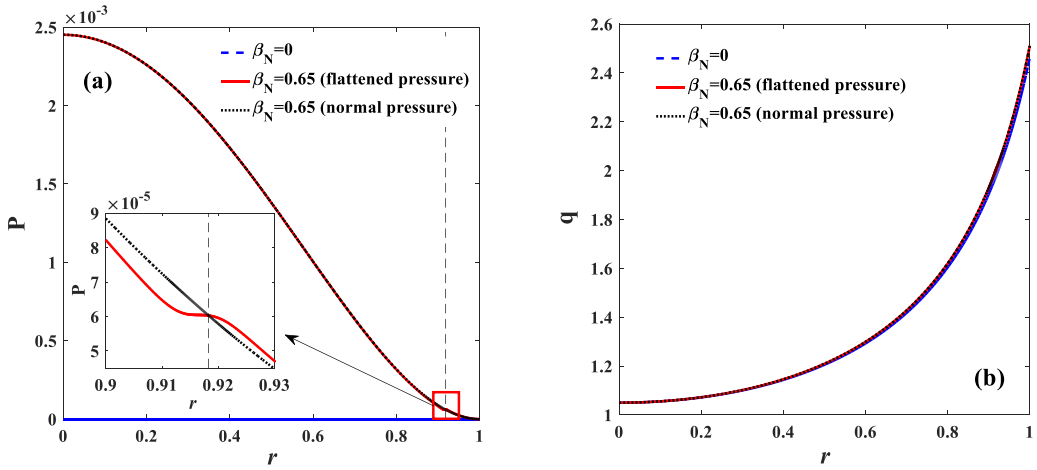

Figure 2. Radial profiles of (a) the equilibrium pressures calculated in CHEASE [35] and (b) the safety factors with fixed on-axis value of $q_0 = 1.05$, assuming three equilibria: $\beta_N = 0$, $\beta_N = 0.65$ with and without locally flattened pressure profile near the $q = 2$ rational surface. The plasma pressure is normalized by B_0^2/μ_0.

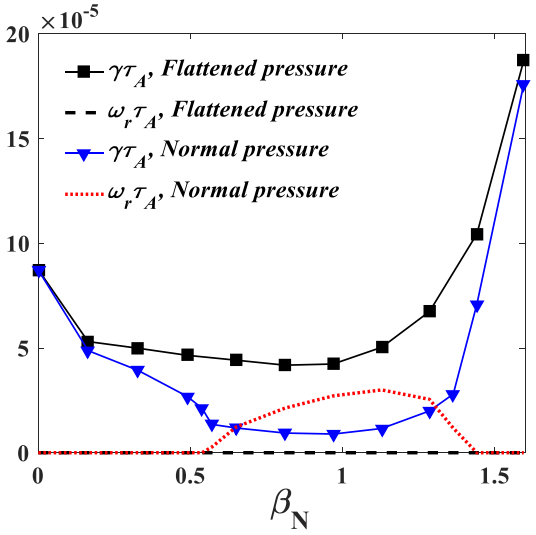

Figure 3. Eigenvalue of the $n = 1$ TM versus the β_N, with or without a locally flattened equilibrium pressure profile near the $q = 2$ rational surface. The Lundquist number is fixed at $S = 5 \times 10^7$.

3.1. Proportional feedback

With a P-controller ($\alpha = 0$) and with increasing feedback gain K_P, the TM is partially or fully stabilized by magnetic control as reported in figure 5(a). Different control configurations (in terms of the choice of active and sensor coils) results in different degree of stabilization. With the same gain value, the strongest stabilization is achieved with the combination of internal (inside the wall) active coils and (internal) poloidal sensors. With this configuration, the critical gain value for full stabilization of the mode is about $K_P = 8.6$ for our equilibrium. Note that the anomaly of the analytic single-pole model [23], showing the best feedback configuration with the combination of external (outside the wall) active coils and (internal or external) poloidal sensors, does not occur with toroidal computations. This is because the MARS-F toroidal modeling includes multiple poloidal harmonics to properly describe the feedback geometry, as explained in [23]. Figure 5(a) also shows that feedback stabilization of the TM is weak with radial sensors.

Figure 5(b) reports the internal (Δ'_{int}) and external (Δ'_{ext}) tearing indices, evaluated based on the MARS-F computed numerical results, versus the feedback gain. As explained before, Δ'_{int} is calculated by inserting the computed mode growth rate (figure 5(a)) into expression (8), where the favorable curvature term and the Pfirsch-Schluter inertial enhancement factor are ignored. Δ'_{ext} is evaluated with expression (7), following the procedure illustrated by figure 4. Figure 5(b) shows that feedback stabilization of the TM is directly related to reduction of the external tearing index, by modifying the external solution in the ideal region outside the resistive layer. The matching condition implies that the inner layer solution has to change to follow the external solution modified by magnetic feedback, which in turn dictates the TM stability. For the equilibrium with vanishing plasma pressure, feedback stabilization of the TM occurs when the external tearing index becomes negative due to the feedback action.

Figure 5(b) also shows a good agreement between Δ'_{int} and Δ'_{ext} as we increase the feedback gain. This is achieved by a proper choice of the $\delta-$parameter when evaluating the derivative jump of the radial field perturbation. It is clear that the $\delta-$value should scale with the resistive layer width, which in turn scales with the TM growth rate as $\gamma^{1/4}$ [36]. Since the close-loop TM growth rate, directly computed by MARS-F, varies with feedback gain, the $\delta-$value for evaluating the logarithmic jump of the external solution should also vary with feedback gain. We thus choose

$$\delta = C(\gamma\tau_A)^{1/4} \tag{9}$$

where C is a constant independent of the feedback gain. C generally depends on the plasma resistivity for a given equilibrium (a more generic scaling is $\delta \sim (\gamma\tau_A/S)^{1/4}$ following in [36]). However, in our case, the plasma resistivity is fixed as we scan

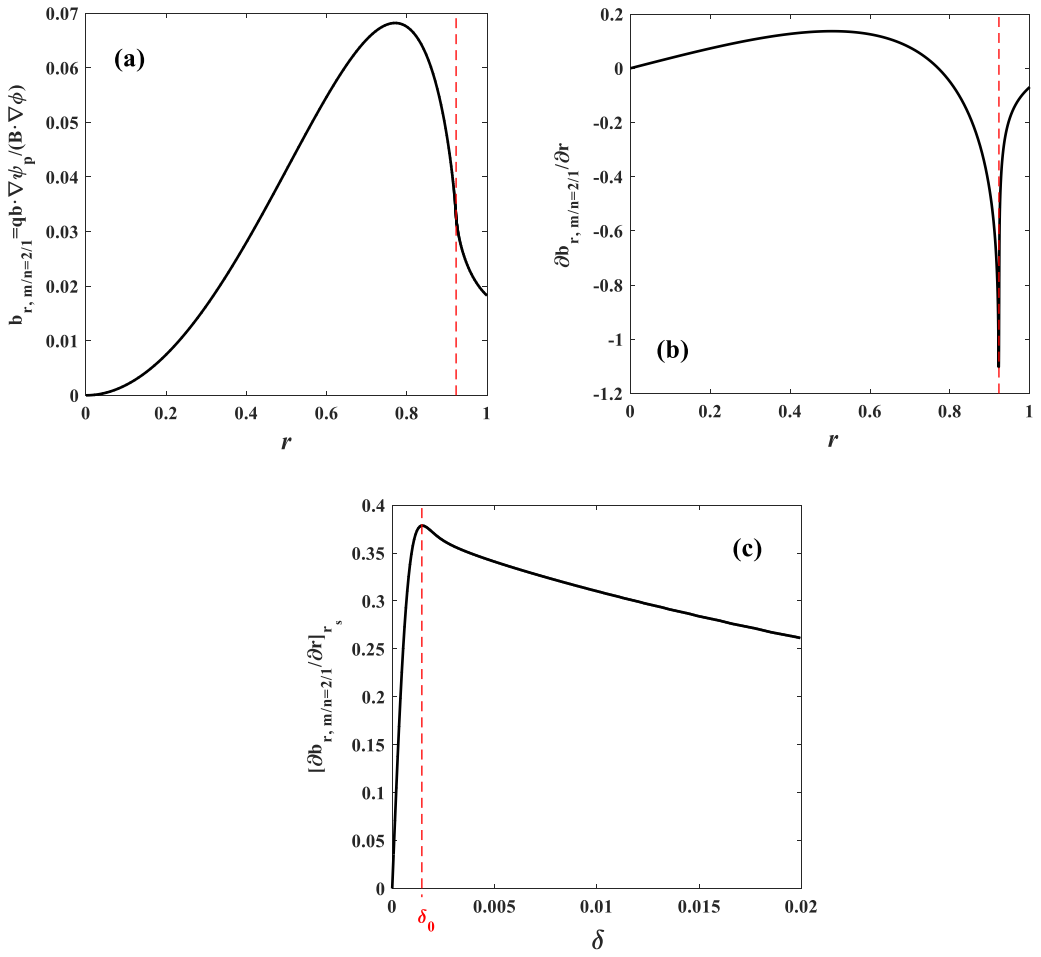

Figure 4. Numerical procedure of evaluating tearing index based on the MARS-F computed TM eigenfunction, showing (a) the $m/n = 2/1$ poloidal harmonic of the perturbed radial magnetic field $b_{r,m/n=2/1} = q\mathbf{b}\cdot\nabla\psi_{\rm P}/(\mathbf{B}\cdot\nabla\varphi)$, (b) the radial derivative of $b_{r,m/n=2/1}$, and (c) the jump in the radial derivative of $b_{r,m/n=2/1}$ when evaluated from both sides of the $q = 2$ surface with distance δ as measured in the radial coordinate r. Vertical dashed lines indicate the location of the $q = 2$ rational surface. The radial distance δ_0 in (c) corresponds to the maximal jump value in the radial derivative. Open loop is assumed here ($G = 0$). An equilibrium with vanishing pressure ($\beta = 0$) is assumed.

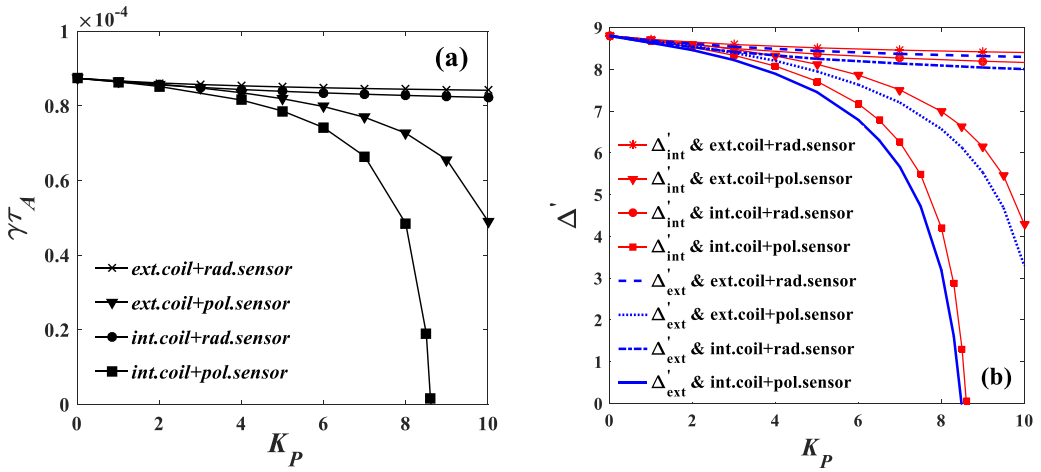

Figure 5. Plotted are (a) growth rate of the $n = 1$ TM, and (b) numerically evaluated $m/n = 2/1$ external ($\Delta'_{\rm ext}$) and internal ($\Delta'_{\rm int}$) tearing indices versus the feedback gain $K_{\rm P}$. Considered is an equilibrium with vanishing pressure ($\beta = 0$). Compared are results with various feedback coil configurations assuming proportional control action alone. Fixed is the plasma resistivity with Lundquist number $S = 5\times10^7$.

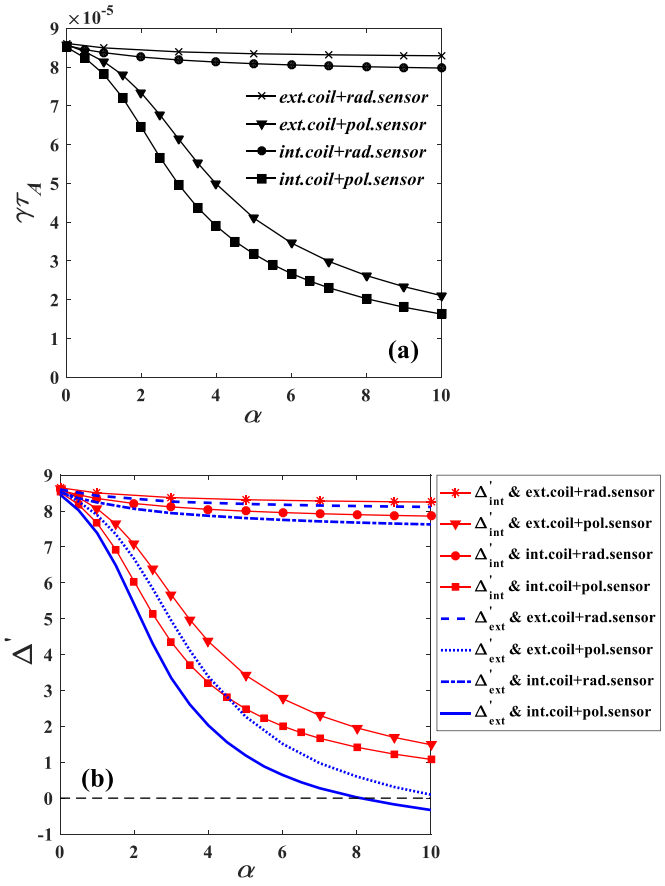

Figure 6. Plotted are (a) growth rate of the $n = 1$ TM, and (b) numerically evaluated $m/n = 2/1$ external ($\Delta'_{\rm ext}$) and internal ($\Delta'_{\rm int}$) tearing indices versus the derivative gain α. Considered is an equilibria with vanishing pressure ($\beta = 0$). Compared are results with various feedback coil configurations assuming proportional derivative control action. Fixed are the amplitude of proportional feedback gain, $K_{\rm P} = 2$, the response time of the active coils, $\tau_{\rm F}/\tau_{\rm w} = 2$, and the plasma resistivity with Lundquist number $S = 5 \times 10^7$.

feedback gain. We fix the C value such that $\Delta'_{\rm int} = \Delta'_{\rm ext}$ for the open-loop, resulting in $C = 0.1$ for the case considered here.

We make two remarks here. (a) The δ-value obtained following the above procedure is the same order of magnitude as the δ_0-value determined by the peaking location shown in figure 4(c). (b) The overall dependence of $\Delta'_{\rm ext}$ on feedback gain is not sensitive to the choice of where the boundary between the inner and outer solutions should be taken (as long as it is not far from δ_0). Therefore, even though it is not possible to exactly define the outer solution based on the MARS-F computed mode eigenfunction, and consequently the exact $\Delta'_{\rm ext}$ value, the qualitative trend of feedback reduction of $\Delta'_{\rm ext}$ is the same. Furthermore, as shown by figure 5(b), quantitative agreement (with $\Delta'_{\rm int}$) for the close-loop follows as soon as we match the external and internal tearing indices for the case of vanishing feedback gain.

3.2. PD feedback

Now we consider a PD-controller. The results reported in figure 6 again assume various combinations of the active and sensor coil types. We fixed the amplitude of the overall feedback gain at $K_{\rm P} = 2$, and vary the derivative gain via the α-parameter as defined in equation (6). The response time of the active coil is also fixed at $\tau_{\rm F}/\tau_{\rm w} = 2$. The combination of internal active coils and poloidal sensors again provides the strongest stabilization to the TM with the derivative action, although no full stabilization is achieved with the PD-controller at fixed $K_{\rm P} = 2$ in our case (figure 6(a)). This is due to the fact that the stabilizing effect of the derivative action diminishes as the mode approaches the marginal stability point.

Expressions (7) and (8), again ignoring the favorable curvature term and the inertial enhancement factor, allow us to obtain the external and internal tearing indices (figure 6(b)), based on the MARS-F close-loop stability results. Note that we choose the same parameter $C = 0.1$ for evaluating δ and $\Delta'_{\rm ext}$ here. Generally good agreement is again obtained between $\Delta'_{\rm ext}$ and $\Delta'_{\rm int}$. The agreement becomes worse at large values of derivative gain, largely due to the uncertainty in determining the exact boundary between the inner and outer solutions as discussed before. The key conclusion from figure 6(b), however, is that derivative action also helps to reduce the external tearing index, and consequently to stabilize the TM.

Similar conclusion is obtained with figure 7, where we again vary the derivative gain but now assuming different values of proportional gain values. Fixed here is the feedback configuration with internal active coils and poloidal sensors. Agreement between $\Delta'_{\rm ext}$ and $\Delta'_{\rm int}$ is still reasonable at small derivative gain. More importantly, figure 7 again confirms that feedback stabilization of the TM largely stems from reduction of the external tearing index. The overall shapes of the growth rate curves (figure 7(a)) and the tearing index curves (figure 7(b)) agree well.

4. Close-loop TM stability and Δ' for equilibrium with finite pressure

In this section, we consider two finite pressure equilibria, both with $\beta_{\rm N} = 0.65$. One equilibrium has a normal pressure profile with finite gradient across the plasma column. The other has locally vanishing pressure gradient across the $q = 2$ surface. For the normal pressure profile case, the external tearing index cannot be evaluated via the logarithmic derivative of the perturbed radial field component, i.e. via the procedure illustrated by figure 4. This is because, in this case, the MHD solution from the outer ideal region has both small (regular) and large (singular) branches near the mode rational surface and the external tearing index is defined as the ratio of the coefficients for the small to large solutions [5]. Such solutions cannot be accurately calculated by MARS-F code in a toroidal geometry. Therefore, we shall only report the internal tearing index for this case. The external tearing index will instead be evaluated using the equilibrium with locally flattened pressure profile (where the favorable curvature effect associated with the inner layer solution again vanishes), following an approach similar to that reported in [13].

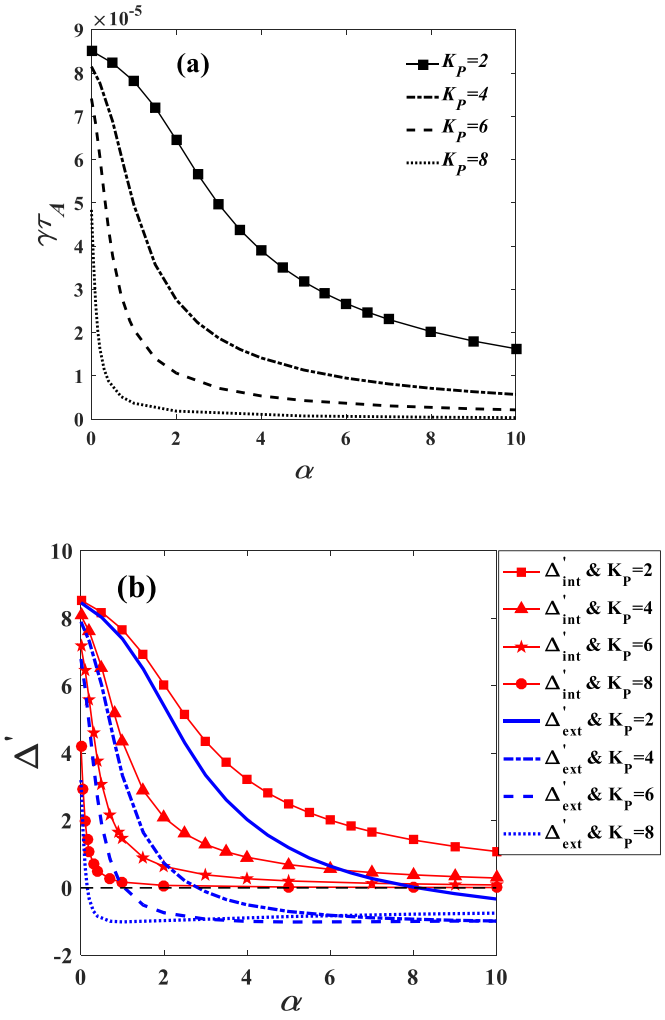

Figure 7. Plotted are (a) growth rate of the $n = 1$ TM, and (b) numerically evaluated $m/n = 2/1$ external ($\Delta'_{\rm ext}$) and internal ($\Delta'_{\rm int}$) tearing indices versus the derivative gain for the different amplitude of feedback gain $K_{\rm P}$. Assumed is the proportional derivative feedback control configuration combining the internal active coils with poloidal sensor. The plasma equilibria pressure and the other parameters are same as that in figure 6.

The key point to realize here is that local modification of the pressure profile, within the inner layer, does not affect the external tearing index, assuming that the local pressure flattening does not significantly change the global profile for the safety factor in a consistent equilibrium, which holds for our case as shown in figure 2. This means that we should expect to obtain the same (internal and external) tearing indices for both equilibria considered here. The situation is, however, slightly more complicated due to different ways of interaction between the feedback system and the wall eddy current response, for both equilibria. This will be further illustrated later on.

As in section 3, we again fix the Lundquist number at $S = 5 \times 10^7$. Considered are again feedback schemes with P- and PD-control.

4.1. Proportional feedback

We start by considering the equilibrium with locally flattened pressure profile, with feedback results reported in figure 8. First, we note that feedback stabilization of the TM becomes stronger in the plasma with finite pressure, with all feedback configurations (figure 8(a)). The combination of internal active coils with poloidal sensors still provides the best result, with full stabilization of the TM occurring as the proportional gain value exceeds 6.5. On the other hand, the mode stabilization is remarkably better with the control schemes assuming radial sensors, compared to the results for the vanishing pressure equilibrium reported in section 3. Note that the close-loop eigenvalue has vanishing imaginary part (i.e. a purely growing instability) for the equilibrium considered here, in the absence of plasma equilibrium flow.

Feedback modification of tearing indices, reported in figure 8(b), again shows good correlation with the TM stability shown in figure 8(a), indicating that feedback action primarily changes the outer solution for the TM. The external tearing index is again evaluated via expression (7), and the coefficient C from equation (9) is chosen to be $C = 0.013$ for this new equilibrium. The internal tearing index is calculated with expression (8), ignoring the favorable curvature term while keeping the inertial enhancement factor. Figure 8(b) again shows good agreement between $\Delta'_{\rm ext}$ and $\Delta'_{\rm int}$, as we vary the proportional feedback gain.

Next, we consider the equilibrium with normal pressure profile, with results reported in figure 9. For this equilibrium, the open-loop TM has finite mode frequency (figure 3) due to the favorable average curvature effect. Proportional feedback action reduces the mode growth rate while further increases the mode frequency (figure 9(a)). Based on the MARS-F computed close-loop eigenvalue, the internal tearing index, $\Delta'_{\rm int}$, is calculated using the full TM dispersion relation (8). The resistive interchange index ($D_{\rm R} = -8.69 \times 10^{-3}$) and the extra correction factor associated with finite plasma pressure ($g \approx 0.58$) are obtained from the CHEASE [35] results. The internal tearing index, calculated this way, has a dominant real part but also a small imaginary part, as shown in figures 9(b) and (c), respectively. (Note that $\Delta'_{\rm int}$ is real at vanishing gain value.) The imaginary part of $\Delta'_{\rm int}$ in the closed loop partly comes from the interaction between feedback and the resistive wall response, where the potential energy dissipation associated with the wall eddy current can produce complex-valued tearing index [23].

Since for the equilibrium with locally flattened pressure profile, the close-loop TM has vanishing mode frequency and the corresponding tearing indices are always real as shown in figure 8, we can compare the real part of the internal tearing index from figure 9(b) with the former. It is evident that the agreement is qualitatively reasonable but quantitatively not good. Numerically, we find a heuristic way of obtaining quantitative agreement for tearing indices between these two equilibria (with and without local pressure flattening), by considering the weighted sum $\mathrm{Re}\,[\Delta_{\rm int}{}'] + D\mathrm{Im}\,[\Delta_{\rm int}{}']$ for the case with complex $\Delta'_{\rm int}$. With a proper choice of the D-value ($D \approx 6.5$ in our case), we obtain good agreement between the weighted sum for the equilibrium with normal pressure profile, and $\Delta'_{\rm int}$ for the equilibrium with locally flattened pressure profile (figure 9(d)). We emphasize that there is no rigorous argument that the weighted sum should be used here for the

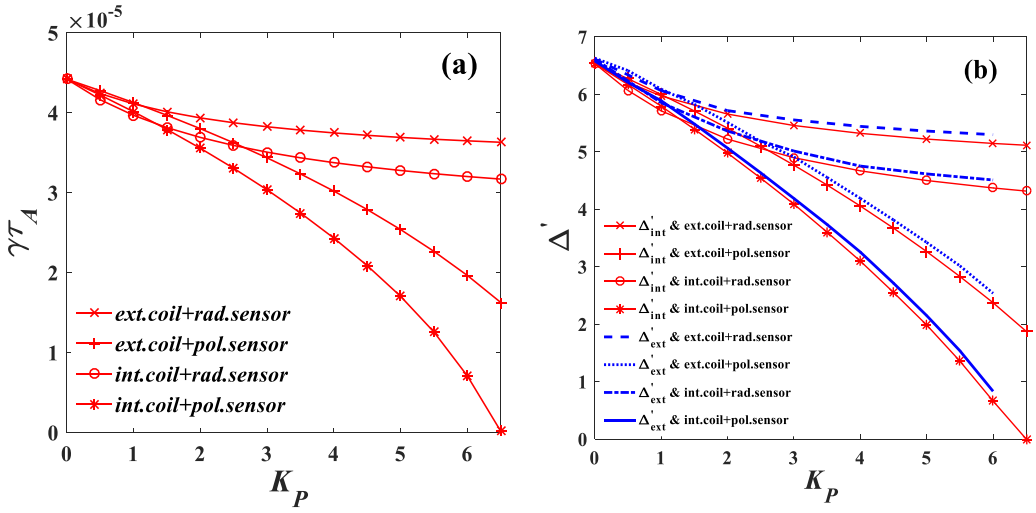

Figure 8. Plotted are the (a) growth rate of the $n = 1$ TM, and (b) numerically evaluated $m/n = 2/1$ external ($\Delta'_{\rm ext}$) and internal ($\Delta'_{\rm int}$) tearing indices versus the amplitude of feedback gain $K_{\rm P}$. Considered is a finite equilibria pressure ($\beta_{\rm N} = 0.65$) profile with locally flattened near the rational surface. Again compared are results with various feedback coil configurations assuming proportional control action alone.

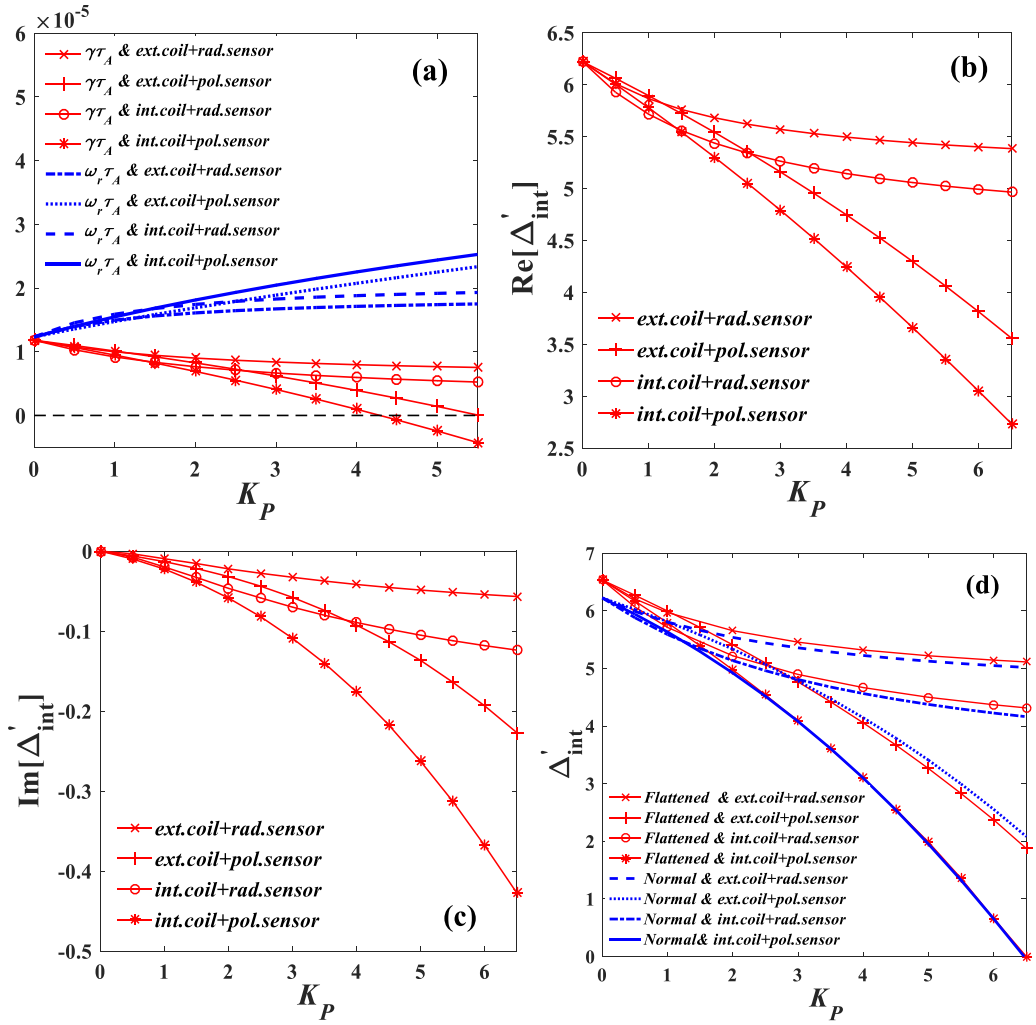

Figure 9. Plotted are the (a) eigenvalues of the $n = 1$ TM, and numerically evaluated (b) real and (c) imaginary part of $m/n = 2/1$ internal ($\Delta'_{\rm int}$) tearing index, versus the amplitude of feedback gain $K_{\rm P}$, by considering a normal finite equilibria pressure ($\beta_{\rm N} = 0.65$) profile. The (d) sum of real and imaginary of $\Delta'_{\rm int}$ for the different finite pressure profiles. Again compared are results with various feedback coil configurations assuming proportional control action alone.

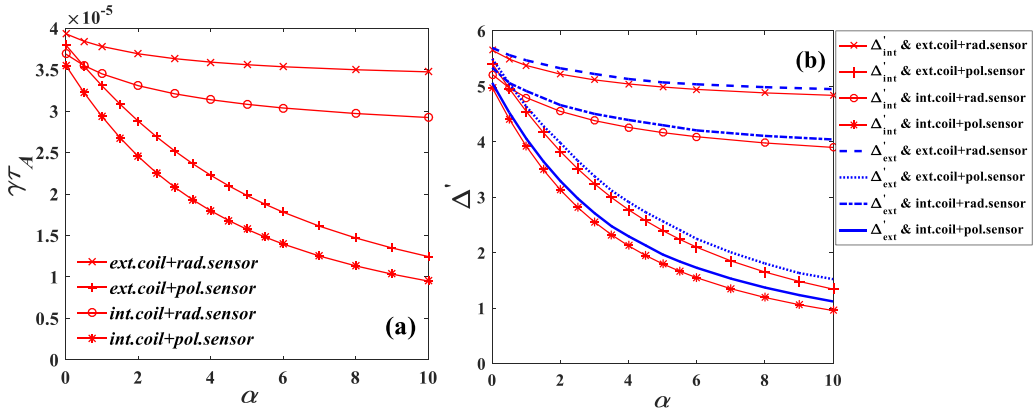

Figure 10. Plotted are the (a) growth rate of the $n = 1$ TM, and (b) numerically evaluated $m/n = 2/1$external ($\Delta'_{\rm ext}$) and internal ($\Delta'_{\rm int}$) tearing indices versus the derivative gain α, by fixing the amplitude of feedback gain, $K_{\rm P} = 2$, and the response time of the active coils, $\tau_{\rm F}/\tau_{\rm w} = 2$. Considered is a finite equilibria pressure ($\beta_{\rm N} = 0.65$) profile with locally flattened near the rational surface. Compared are results with various feedback coil configurations assuming proportional derivative control action.

comparison, besides an intuitive understanding that the tearing index generally represents free energy that drives the TM, and the weighted sum in certain sense represents the total perturbed energy associated with the mode.

4.2. PD feedback

We now report feedback results with a PD-controller for these two finite pressure equilibria. We fix the proportional gain at $K_{\rm P} = 2$ and scan the derivative gain. Results for the equilibrium with locally flattened pressure profile are summarized in figure 10. Similar to the case with vanishing equilibrium pressure as reported in section 3, figure 10(a) shows partial stabilization of the TM by the derivative action. This is directly related to partial reduction of the tearing index as shown in figure 10(b). Furthermore, figure 10(b) again demonstrates good match of tearing indices evaluated from the inner and outer solutions, respectively, in the presence of a PD-controller.

PD-feedback results for the equilibrium with normal pressure profile are reported in figure 11. The derivative action again stabilizes the TM. In particular, the feedback configuration with internal active coils and poloidal sensors allows full stabilization of the mode at sufficiently large derivative gain, contrary to the case shown in figure 10(a). This is because the derivative action is effective even close to the mode marginal stability when the mode frequency remains finite, which is the case for the equilibrium considered here. As mentioned before, the finite mode frequency is introduced by the favorable curvature effect (in the absence of equilibrium flow), and the feedback action further modifies the mode frequency. In particular, we find that the derivative action increases the mode frequency with radial sensors, and reduces the mode frequency with poloidal sensors.

The real and imaginary parts of the inner tearing index, evaluated from the close-loop TM eigenvalue, are reported in figures 11(b) and (c), respectively. It is interesting to note that with radial sensors, derivative gain reduces ${\rm Re}\,[\Delta'_{\rm ext}]$, while the opposite trend holds with poloidal sensors. On the other hand, ${\rm Im}\,[\Delta'_{\rm int}]$ is always reduced by the derivative action. Furthermore, the weighted sum of the real and imaginary parts of the inner tearing index, ${\rm Re}\,[\Delta_{\rm int}{}'] + D{\rm Im}\,[\Delta_{\rm int}{}']$, again recovers well that calculated for the equilibrium with locally flattened pressure profile (figure 11(d)), by choosing $D \approx 2.5$.

5. Conclusion and discussion

We have numerically investigated magnetic feedback stabilization of the TM utilizing the MARS-F code for toroidal tokamak equilibria. Considered are three types of equilibria: with vanishing pressure, with finite pressure but locally finite versus zero pressure gradient at the mode rational surface. Assumed is either P- or PD-controller and compared are different feedback coil configurations. Our emphasis is on understanding how magnetic feedback affects tearing indices.

We find that magnetic feedback generally (partially or fully) stabilizes the TM in a tokamak plasma, independent of the feedback coil configuration and the type of plasma equilibrium. The best control is offered by the combination of internal active coils and internal poloidal sensors. The derivative action further enhances the mode stabilization. For equilibria where the favorable curvature stabilization is not important, the close-loop eigenvalue is a real number (i.e. a purely growing instability) and the derivative action does not lead to full stabilization of the TM. The latter, however, can occur for equilibria with finite pressure gradient at the mode rational surface, thanks to the finite mode frequency even at the marginal stability point.

Whilst the internal tearing index can be straightforwardly calculated based on the MARS-F computed close-loop eigenvalue, evaluation of the external tearing index, based on the MARS-F computed mode eigenfunction, requires careful determination of the boundary between the inner and outer solutions. This is achieved by taking into account the analytic scaling of the inner layer width with the close-loop growth rate, equation (9), where the coefficient C is numerically

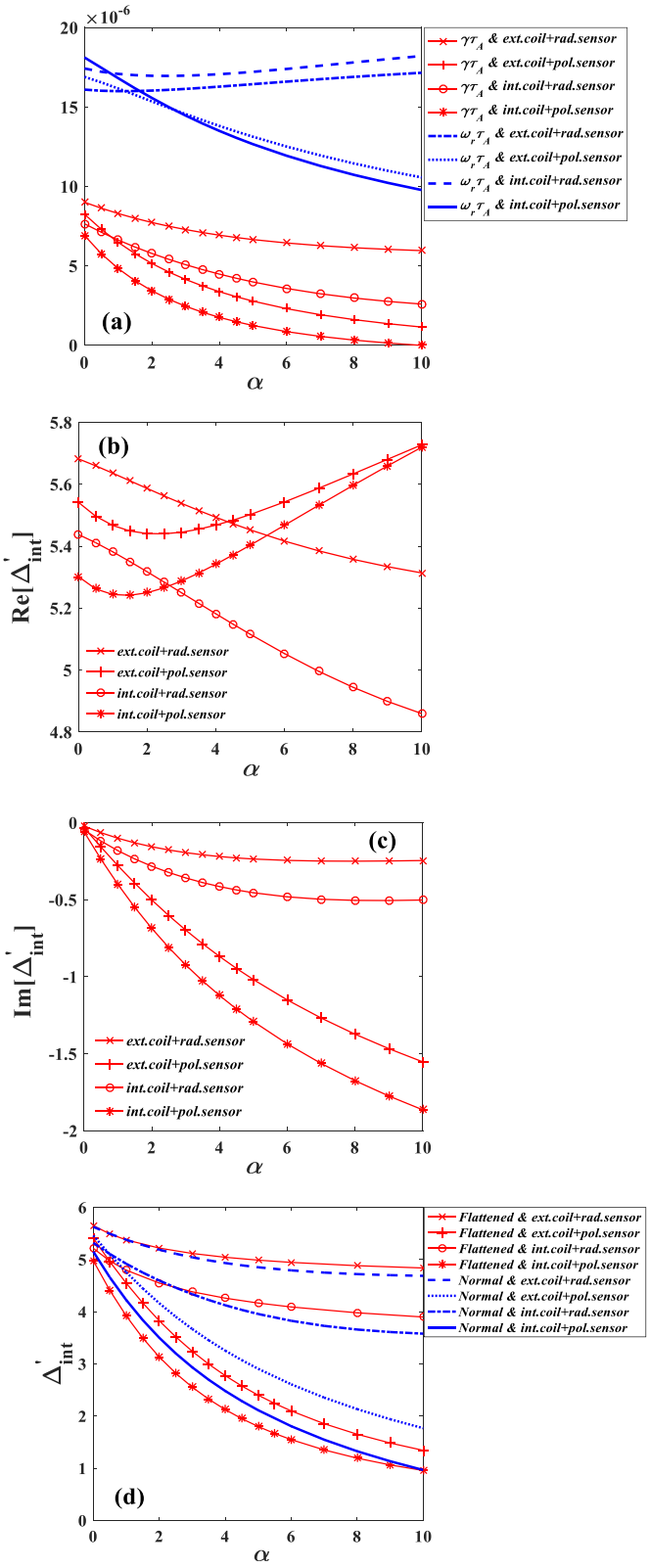

Figure 11. Plotted are the (a) eigenvalues of the $n = 1$ TM, and numerically evaluated (b) real and (c) imaginary part of $m/n = 2/1$ internal ($\Delta'_{\rm int}$) tearing index, versus the derivative gain α, by considering a normal finite equilibria pressure ($\beta_{\rm N} = 0.65$) profile. The (d) sum of real and imaginary of $\Delta'_{\rm int}$ for the different finite pressure profiles. Again compared are results with various feedback coil configurations assuming proportional derivative control action.

determined by matching the internal and external tearing indices at vanishing feedback gain (i.e. open-loop). The C value depends on the plasma equilibrium and the plasma resistivity but is kept constant while scanning the feedback gain.

In the absence of the favorable curvature effect, both the internal and external tearing indices are calculated as real numbers and quantitatively agree well with each other. For the equilibrium with finite pressure gradient at the mode rational surface, the favorable average curvature effect becomes important. Both the open-loop and close-loop eigenvalues become complex (for certain range of the plasma pressure). The close-loop tearing index also becomes complex-valued partly due to interaction of the feedback system with the dissipative wall eddy current response. A heuristic model, based on weighted sum of the real and imaginary parts of the internal tearing index, allows restoring a real tearing index that agrees well with the value obtained for the plasma without favorable curvature effect.

Our toroidal modeling shows that active control of the TM, with either P- or PD-control, is directly correlated to the magnetic feedback modification of the solution in the outer ideal plasma region, thus confirming the early idea proposed in [33]. In other words, feedback stabilizes the TM by mainly modifying the behavior of the external ideal solution outside the resistive layer.

Combination of the previous analytic work from [23, 33] and the present numerical study provides a solid theoretical basis for interpreting feedback control of the TM via magnetic means. Because the results show that feedback modification of the external tearing index plays a dominant role in the close-loop stability, the same technique can also be applied to control the NTM. Presently, NTM control mainly relies on non-magnetic means such as the electron cyclotron current drive in tokamak devices. Magnetic control can provide a complementary method here and further efforts are desirable. In particular, the effect of plasma toroidal flow on the close-loop stability needs to be investigated. Toroidal modeling of magnetic feedback control of TM for realistic experiments also remains a future study.

Data availability statement

The data that support the findings of this study are available upon reasonable request from the authors.

Acknowledgments

This work is funded by National Natural Science Foundation of China (NSFC) (Grant Nos. 11905067, 11847219 and 11905022), and the China Postdoctoral Science Foundation under Grant No. 2019M652931. The work is also supported by the U.S. DoE Office of Science under Contract Nos. DE-FG02–95ER54309 and DE-FC02–04ER54698. The work is also supported by Chongqing Basic Research and

Frontier Exploration Project in 2019 (Chongqing Natural Science Foundation: cstc2019jcyj-msxmX0567) and the Science and Technology Research Program of Chongqing Municipal Education Commission (Grant No. KJQN201900819).

ORCID iDs

Yuling He https://orcid.org/0000-0002-9765-227X
Yueqiang Liu https://orcid.org/0000-0002-8192-8411

References

[1] Furth H P, Killeen J and Rosenbluth M N 1963 *Phys. Fluids* **6** 459
[2] La Haye R J 2006 *Phys. Plasmas* **13** 055501
[3] Turco F and Luce T C 2010 *Nucl. Fusion* **50** 095010
[4] Furth H P, Rutherford P H and Selberg H 1973 *Phys. Fluids* **16** 1054
[5] Glasser A H, Greene J M and Johnson J L 1975 *Phys. Fluids* **18** 875
[6] Glasser A H, Greene J M and Johnson J L 1976 *Phys. Fluids* **19** 567
[7] He Y L, Liu Y Q, Liu Y, Hao G Z and Wang A K 2014 *Phys. Rev. Lett.* **113** 175001
[8] He Y L, Liu Y Q, Liu Y, Liu C, Xia G L, Wang A K, Hao G Z, Li L and Cui S Y 2016 *Phys. Plasmas* **23** 012506
[9] Coppi B, Greene J M and Johnson J L 1966 *Nucl. Fusion* **6** 101
[10] Connor J W, Cowley S C, Hastie R J, Hender T C, Hood A and Martin T J 1988 *Phys. Fluids* **31** 577
[11] Bishop C M, Connor J W, Hastie R J and Hastie S C 1991 *Plasma Phys. Control. Fusion* **33** 389
[12] Nishimura Y, Callen J D and Hegna C C 1998 *Phys. Plasmas* **5** 4292
[13] Ham C J, Connor J W, Cowley S C, Hastie R J, Hender T C and Liu Y Q 2013 *Plasma Phys. Control. Fusion* **55** 125015
[14] Hender T C, Hastie R J and Robinson D C 1987 *Nucl. Fusion* **27** 1389
[15] Fitzpatrick R, Hastie R J, Martin T J and Roach C M 1993 *Nucl. Fusion* **33** 1533
[16] Ham C J, Connor J W, Cowley S C, .Gimblett C G, Hastie R J, Hender T C and Martin T J 2012 *Plasma Phys. Control. Fusion* **54** 025009
[17] Ham C J, Liu Y Q, Connor J W, Cowley S C, Hastie R J, Hender T C and Martin T J 2012 *Plasma Phys. Control. Fusion* **54** 105014
[18] Liu Y Q, Bondeson A, Fransson C M, Lennartson B and Breitholtz C 2000 *Phys. Plasmas* **7** 3681
[19] Finn J, M 2006 *Phys. Plasmas* **13** 082504
[20] Liu Y Q, Hastie R J and Hender T C 2012 *Phys. Plasmas* **19** 092510
[21] Brennan D P and Finn J M 2014 *Phys. Plasmas* **21** 102507
[22] Zanca P, Paccagnella R, Finotti C, Fassina A, Manduchi G, Cavazzana R, Franz P, Piron C and Piron L 2015 *Nucl. Fusion* **55** 043020
[23] He Y L, Liu Y Q, Yang X, Xia G L and Li L 2021 *Phys. Plasmas* **28** 012504
[24] Hender T C *et al* 2007 *Nucl. Fusion* **47** S128
[25] Wan Y X *et al* 2017 *Nucl. Fusion* **57** 102009
[26] Strait E J 2015 *Phys. Plasmas* **22** 021803
[27] Liu Y Q and Bondeson A 2000 *Phys. Rev. Lett.* **84** 907
[28] Liu Y Q *et al* 2005 *Nucl. Fusion* **45** 1131
[29] Hao G Z, Liu Y Q, Wang A K, Xu M, Qu H P, Peng X D, Wang Z H, Xu J Q and Qiu X M 2014 *Phys. Plasmas* **21** 012503
[30] Liu Y Q, Connor J W, Cowley S C, Ham C J, Hastie R J and Hender T C 2012 *Phys. Plasmas* **19** 072509
[31] Li L, Liu Y Q, Huang X, Luan Q and Zhong F C 2017 *Phys. Plasmas* **24** 020705
[32] Yang X, Liu Y Q, Paz-Soldan C, Zhou L N, Li L, Xia G L, He Y L and Wang S 2019 *Nucl. Fusion* **59** 086012
[33] Arsenin V V 1977 *Proc. 8th European Conf. Controlled Fusion and Plasma Physics Contributed Papers* (*Prague*) vol I p 43
[34] Smolyakov A I, Hirose A, Lazzaro E, Re G B and Callen J D 1995 *Phys. Plasmas* **2** 1581
[35] Lutjens H, Bondeson A and Sauter O 1996 *Comput. Phys. Commun.* **97** 219
[36] White R B 2008 *AIP Conf. Proc.* **1013** 59